

Peripapillary Intravitreal Injection Improves AAV-Mediated Retinal Transduction

Sanjar Batirovich Madrakhimov,^{1,2} Jin Young Yang,^{1,2} Dong Hyuck Ahn,² Jung Woo Han,³ Tae Ho Ha,⁴ and Tae Kwann Park^{1,2,3,5,6}

¹Department of Interdisciplinary Program in Biomedical Science, Soonchunhyang Graduate School, Bucheon Hospital, Bucheon, South Korea; ²Laboratory for Translational Research on Retinal and Macular Degeneration, Soonchunhyang University Hospital Bucheon, Bucheon, South Korea; ³Department of Ophthalmology, Soonchunhyang University Hospital Bucheon, Bucheon, South Korea; ⁴CMLAB, Convergence Technologies for Bio-Medical Science, Seoul, South Korea; ⁵Department of Ophthalmology, College of Medicine, Soonchunhyang University, Cheonan, Choongchungnam-do, South Korea; ⁶Ex Lumina Therapeutics and Technologies, Bucheon, South Korea

The intravitreal (IVT) injection method is a choice when targeting the inner retina for gene therapy. However, the transduction efficiency of adeno-associated virus (AAV) vectors administered by the IVT route is usually low and may be affected by several factors. To improve the transduction efficiency, we developed a novel illuminated long-needle attached injection system and injected AAV2-CMV (cytomegalovirus)-EGFP in front of the retina in rabbit eyes. Ophthalmological examinations were performed and the levels of pro-inflammatory cytokines in the aqueous humor were assessed at the baseline and 1 month, and the results were compared with those of the conventional injection method. Retinal tissues were used for immunohistochemistry. In the ophthalmological examinations, no significant inflammatory signs were detected in both groups, except for transient, mild hyperemia. In the tissues of the rabbits in the peripapillary injection group, significantly increased GFP expression was detected at the ganglion cell and the inner nuclear layers ($p < 0.01$). There were no differences between groups in glial activation and expressions of interleukin (IL)-6 and IL-8. These results suggest that peripapillary IVT injection in front of the retina would be safe and efficiently transduce viral vectors into the retina of large animals and is considered as a potential method for use in clinical trials.

INTRODUCTION

Gene transfer strategy is a promising approach to treat inherited and acquired retinal disorders. Several clinical trials have demonstrated the therapeutic potential of viral vector-mediated gene transfer for the treatment of Leber congenital amaurosis,^{1,2} retinitis pigmentosa,³ choroideremia,^{4–6} and age-related macular degeneration,⁷ and the range of indications approved for gene therapy trials is increasing⁸. These clinical trials utilized adeno-associated virus (AAV) to deliver the gene of interest to the retina. AAV vectors derived from non-pathogenic parvovirus emerged as the predominant vehicles for gene delivery because of their minimal immunogenicity, long-term gene expression in dividing and terminally differentiated cells, and wide range of host and cellular tropism.^{9,10}

Two main routes of AAV administration are used to target the retina—subretinal and intravitreal (IVT). The subretinal route involves an injection of viral vector into the potential space between photoreceptors and retinal pigment epithelium (RPE) with the risk of potential complications, such as retinal thinning, inflammation, recurrent retinal detachment, and choroidal effusion.^{1,6,11} IVT injection is a widely used method in clinical practice as a relatively safe method to deliver various therapeutic agents, including viral vectors.^{12–18} However, the transduction efficiency of viral vectors administered by IVT injection may be affected by several factors, including, but not limited to, the vitreous humor, inner limiting membrane (ILM), retinal extracellular matrix and cell surface proteoglycans.^{19–21} Improvement of retinal gene transduction using extracellular matrix-degrading enzymes^{19,20,22} or surgical interventions such as vitrectomy²³ and/or ILM peeling²¹ have been reported. However, the proposed solutions harbor a risk of ocular adverse effects: enzymatic vitreolysis may lead to functional and structural changes in the retina due to the diffuse protease effect,^{20,24,25} and surgical manipulations may potentially be accompanied by complications related to additional surgical procedures.

Different approaches were evaluated to augment the retinal transduction of AAV vectors. Recently, we reported the improvement of AAV-mediated retinal transduction by prior laser photocoagulation of the mouse retina *in vivo*.²⁶ In the current study, to enhance the retinal transduction of AAV vector, we took into account the needle parameters and depth of insertion, as they are considerable factors in terms of the effectiveness of therapeutic agents delivered by the IVT route.^{12,27} The correlation was observed between the depth of insertion of the needle and treatment outcomes.^{12,27,28} There is no consensus regarding the needle gauge and length for IVT injection.^{12,27} The commonly used needle size in clinical practice ranges

Received 12 February 2020; accepted 23 March 2020;
<https://doi.org/10.1016/j.omtm.2020.03.018>.

Correspondence: Tae Kwann Park, MD, PhD, Department of Ophthalmology, Soonchunhyang University Hospital Bucheon, #170, Jomaru-ro, Wonmi-gu, Bucheon 14584, South Korea.
E-mail: tkpark@schmc.ac.kr



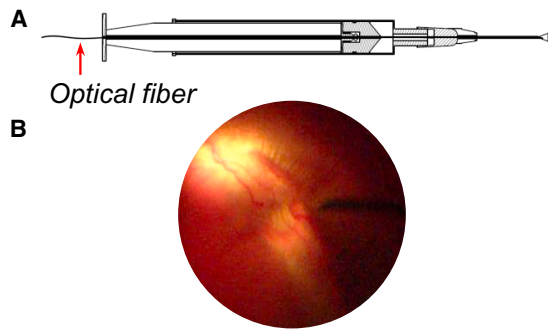


Figure 1. A Novel Illuminated Long-Needle Attached Injection System

(A) Schematic of a novel illuminated long-needle attached injection system with a light source. (B) Peripapillary injection of the viral vector using the novel injection system under direct visualization of the fundus.

from 27G to 30G and 8 to 13 mm in length.^{12,29,30} We hypothesized that delivering the vector close to the retina (peripapillary injection) using a novel injection system under direct visualization would improve the transduction efficacy of viral vector. To test our hypothesis, we compared the transduction efficacy and safety profile of peripapillary IVT injection of AAV2-CMV-EGFP using a novel injection system constructed with an optical fiber inside a 27G (25-mm) needle-attached syringe and a conventional IVT injection (27G [13 mm]) in rabbit eyes (Figure 1).

RESULTS

Clinical Examination

Examination of the anterior segment of rabbit eyes before injection revealed one eye with grade 2 conjunctival hyperemia in rabbits of both the conventional and peripapillary injection groups, and other eyes demonstrated grade 0 or 1 hyperemia. At 2 weeks, grade 2 conjunctival hyperemia was observed in three eyes of rabbits in both groups. At 4 weeks, all eyes of rabbits in the conventional injection group showed grade 0 or 1 hyperemia, while one eye of a rabbit in the peripapillary injection group treated with viral vector still had mild hyperemia (Figure 2A).

At weeks 2 and 4 post-injection, grade 1 and 2 vitreous opacities were observed in both groups of rabbits. However, balanced salt solution (BSS)-injected eyes demonstrated less vitreous abnormalities than did AAV2-injected eyes in both groups ($p > 0.05$). Vitreous opacities were mostly located peripapillary and/or in the central vitreous in rabbit eyes that received AAV2 (Figure 2B).

In Vivo Imaging of GFP Fluorescence

Fundus imaging of AAV2-injected rabbit eyes in the conventional injection group showed a few scattered GFP fluorescent signals on the 2nd week of observation (Figure 3D2). At 4 weeks, GFP fluorescence appeared as an accumulation of signal in some parts of the retina (Figure 3D3). Autofluorescence (AF) images of AAV2-injected rabbit eyes in the peripapillary injection group showed the homogeneous distribution of GFP signal throughout the retina at 2 weeks of observation, and the signal intensity was enhanced at 4 weeks (Figures

3E1–3E3). Fundus images of rabbits before injection and vehicle-injected eyes at 4 weeks served as control (Figures 3A–3C).

Histologic Examination

Confocal microscopy of flat mounts of retinas following AAV2 injection via the conventional technique resulted in a sparse and low-intensity fluorescence mostly limited to the ganglion cell layer (GCL) and barely found in the inner nuclear layer (INL) (Figure 4A). The peripapillary injection technique increased the depth of retinal transduction. The analysis of confocal slices at the level of GCL following peripapillary injection revealed an evenly distributed strong fluorescent signal from structures resembling nerve fibers and ganglion cells (Figure 4A). Deeper in the retina, a number of GFP-expressing cells were observed in the INL (Figure 4C). 3D images of rabbit retina demonstrate GFP signals from the full thickness of z-sectioned constructs (Figure 4D). The results of the quantitative analysis of GFP-expressing cells are summarized in Figure 4E.

Furthermore, to evaluate GFP transduction in different retinal layers as well as the cellular tropism based on cell shape and location, cryosections of rabbit retina were analyzed for fluorescence (Figure 5). Cryosections from AAV2-injected rabbit eyes in the conventional injection group showed weak GFP expression in GCL and rarely in INL. Cryosections of AAV2-injected rabbit eyes using the novel injection system demonstrated strong GFP fluorescence and broad cellular tropism including ganglion cells, Müller cells, horizontal cells, and bipolar cells (Figure 5).

Cell-Mediated Local Immune Response

To identify histological changes reflecting a local immune response, we performed immunostaining for glial fibrillary acidic protein (GFAP) and ionized calcium-binding adaptor molecule 1 (Iba1) antibodies. Control rabbit retina demonstrated no GFAP immunoreactivity, as the healthy rabbit retina Müller cells lacked GFAP.^{31–33} AAV2-injected eyes of rabbits in the conventional and peripapillary injection groups demonstrated GFAP immunoreactivity, suggestive of glial activation (Figure 6A). Immunostaining for Iba1 antibody also demonstrated a few amoeboid microglial cells in control retina, whereas Iba1 immunoreactivity in AAV2-injected retinas of rabbits was upregulated in both groups (Figure 6B).

Aqueous Humor Analysis

The total protein level in aqueous humor (AH) obtained from rabbits in the conventional and peripapillary injection group before injection was at a concentration of 4.04 ± 0.5 and 3.21 ± 0.12 mg/mL (mean \pm SEM), respectively. At 2 weeks, virus vector injection resulted in higher levels of the total protein in AH compared to that of vehicle-injected AH in both groups. However, at 4 weeks, total protein level in AH samples from the conventional and peripapillary injection group decreased to the baseline values, that is, 6.96 ± 1.31 and 4.99 ± 0.32 mg/mL, respectively (mean \pm SEM). The changes in the total protein level during the observation period between AAV-administered groups using conventional and peripapillary injection were not significant ($p = 0.965$). AH of lipopolysaccharide

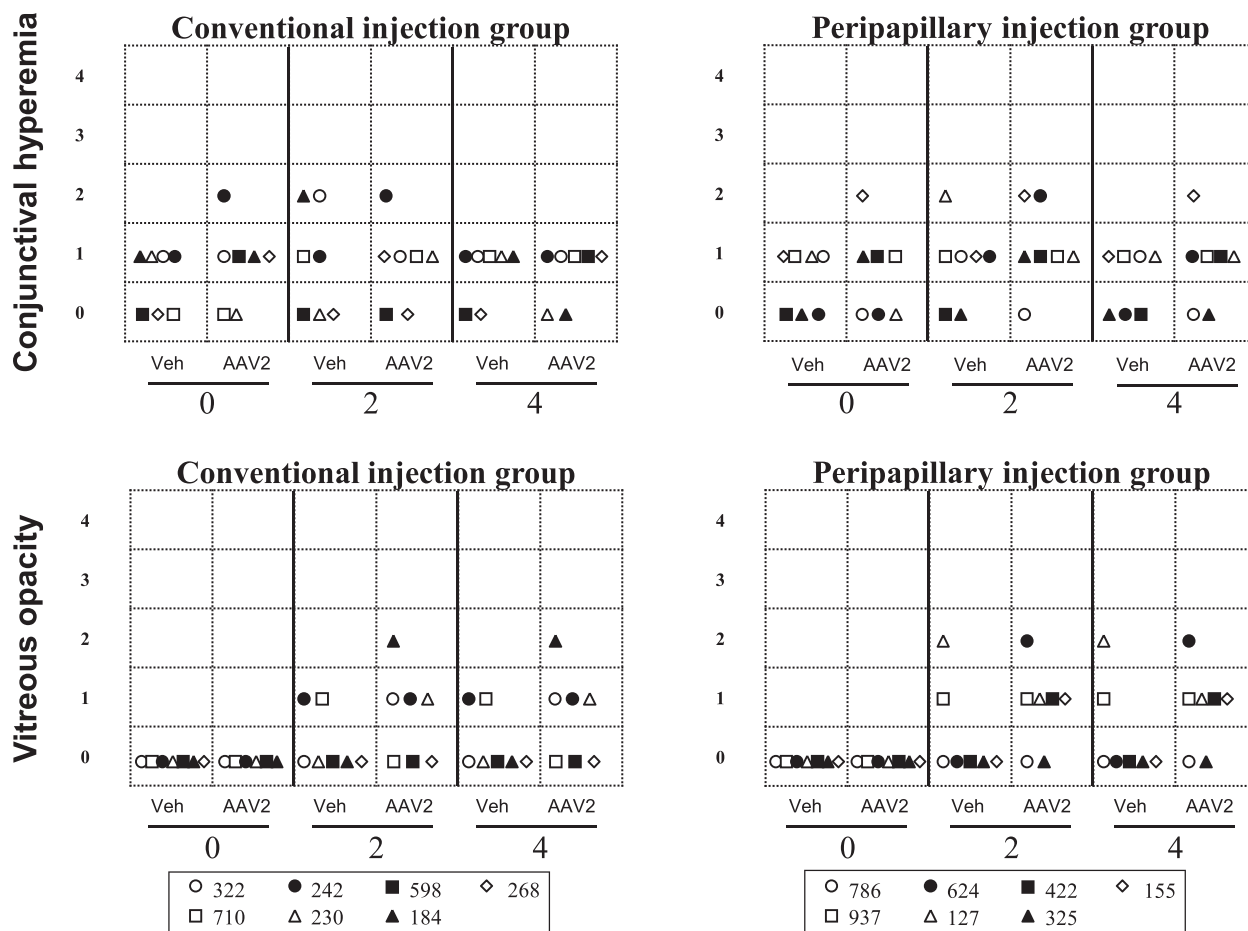


Figure 2. Clinical Findings in Rabbits after Injection of AAV2 EGFP and Vehicle Using Conventional and Peripapillary Injection

The findings from AAV2 or vehicle-injected eyes using conventional and peripapillary injection are presented for each rabbit (n = 7 per group) at 0, 2, and 4 weeks of observation. Symbols represent rabbit IDs: 322, 242, 598, 268, 710, 230, and 184 for the conventional injection group; 786, 624, 422, 155, 937, 127, and 325 for the peripapillary injection group.

(LPS)-treated rabbit eyes demonstrated increased protein content of 15.72 ± 0.08 mg/mL (mean \pm SEM, Figure 7A).

Cytokine levels in AH from rabbits in the conventional and peripapillary injection groups are shown in Figures 7B and 7C. Interleukin (IL)-6 evaluated by ELISA were at minimum detectable levels at baseline (5.6 ± 2.86 pg/mL, mean \pm SEM) and 2 weeks of observation in the AH obtained from rabbits in the conventional injection group (AAV2, 1.62 ± 0.84 pg/mL; vehicle, 11.23 ± 6.05 pg/mL; mean \pm SEM). At 4 weeks, the conventional injection group demonstrated an elevation of IL-6 levels in AH of both AAV2 and vehicle-injected eyes (120.14 ± 5.1 and 133.19 ± 6.6 pg/mL, respectively; mean \pm SEM). The peripapillary injection group showed similar levels of IL-6 at 2 and 4 weeks of injection (Figure 7B). Comparison of two injection groups showed no significant difference in IL-6 levels in AH at post-injection week 4 ($p = 0.158$, Figure 7B). AAV2 administration using the novel injection system resulted in the transient elevation of IL-8 at week 2 post-injection (189.6 ± 10.75 pg/mL), since at week 4 post-

injection, IL-8 expression (79 ± 16.24 pg/mL) was at baseline levels (90.47 ± 5.87 pg/mL, mean \pm SEM). The conventional injection group showed similar levels of IL-8 at each time point in both AAV2 and vehicle-injected eyes (Figure 7C). The difference in IL-8 levels in AH of AAV-administered groups using conventional and peripapillary injection at week 4 post-injection was out of statistical significance ($p = 0.183$). LPS-treated rabbit eyes served as a positive control and demonstrated high levels of IL-6 (676.2 ± 37.03 pg/mL) and IL-8 (360.3 ± 61.2 pg/mL, mean \pm SEM) (Figures 7B and 7C).

DISCUSSION

In this study, we demonstrated that injection of recombinant viral vector close to the retina using an illuminated long-needle attached injection system improves transduction efficacy of AAV2-CMV-EGFP virus. Viral vector effectively transduced retinal ganglion cells, Müller cells, and INL cells. These findings suggest the novel injection system as a potential method of IVT viral vector delivery in clinical trials.

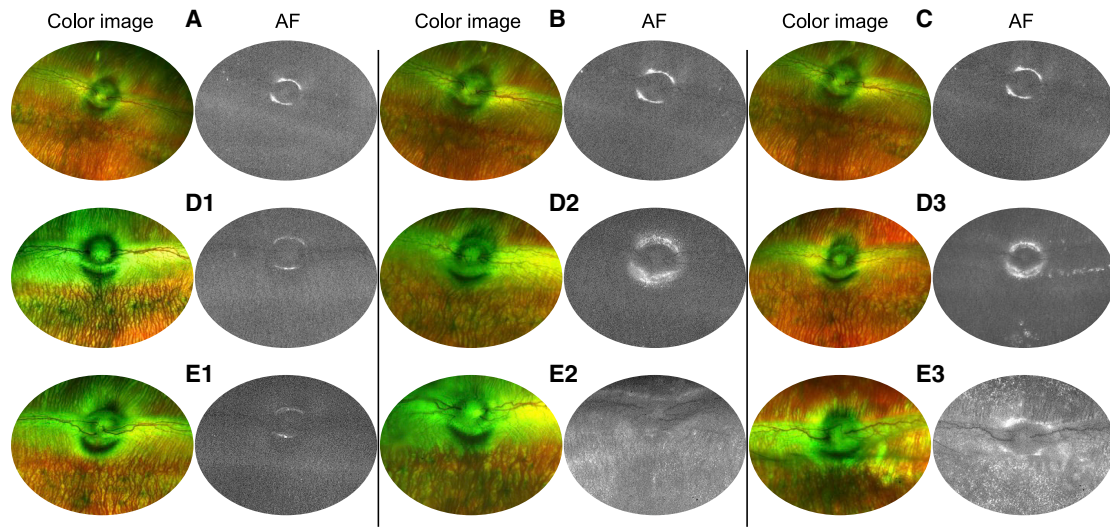


Figure 3. Representative Fundus Images of Rabbit Eyes Injected with AAV2

(A) Color and AF image of rabbit eye before injection. (B) Color and AF images obtained from rabbit eye after 4 weeks of vehicle injection using a conventional method. (C) Color and AF images obtained from rabbit eye after 4 weeks of vehicle injection using the novel system. (D1–D3) Color and AF images of the conventional injection group's rabbit eye before injection (D1) and after 2 (D2) and 4 weeks (D3). (E1–E3) Color and AF images of the peripapillary injection group's rabbit eye before injection (E1) and after 2 (E2) and 4 weeks (E3).

We used recombinant AAV2-CMV-eGFP virus and a rabbit eye model for IVT injection. AAV2 is the most widely studied serotype and is effectively used in many clinical trials.^{1–5,7} In the context of IVT injection, rabbit eyes are a convenient model because of similarity of volume with human eyes and are widely used in gene therapy research.^{13,14,34,35} As a type of minimally invasive intraocular surgery, IVT injections may be complicated by intraocular inflammation. Therefore, we assessed inflammatory response to injection by clinical examination of the conjunctiva and vitreous cavity. Examination of conjunctiva revealed grade 1 and 2 conjunctival hyperemia at different time points, even prior to the surgical procedure, in AAV2 and vehicle-injected eyes of rabbits in both groups. These observations indicate that hyperemia was not associated with the injection procedure and or viral vector administration. Clinical findings of vitreous examination at weeks 2 and 4 post-injection were also limited to grade 1 and 2 vitreous condensations, and vehicle-injected eyes tended to have fewer vitreous opacities when compared with AAV2-injected eyes ($p > 0.05$). The onset of vitreous signs of an inflammatory response to AAV2 administration at 2 weeks indicates that vitreous condensation was related to viral vector, not to the injection procedure. Of note, no morphological changes of the retina were observed on color fundus images during 1 month of observation (Figure 3).

The most common AAV serotypes in clinical use, that is, AAV2 and AAV8, demonstrate limited transduction efficacy restricted to the inner retina when administered IVT.^{36–40} These AAV serotypes have certain capsid properties, which contact with different cell surface receptors to enter the host cell and are a major determinant of its cellular tropism and transduction efficacy.^{41,42} However, the transduction ef-

ficacy of injected viral vector even with rationally designed capsid structure may be reduced by vitreous due to the physical and rheological properties of the latter.^{43–45} Dilution of concentration of injected viral vector in the vitreous,⁴³ and the structural components consisting of collagen and other proteins,⁴⁶ may trap the injected vector and result in uneven distribution, and subsequently low transduction efficacy.²³ Autofluorescence images of rabbit retina that received AAV2 using the conventional technique demonstrated the patchy-like distribution of GFP signal predominantly at the injection site (Figure 3), consistent with the findings in other publications.^{20,38,47,48} Other vitreous-related obstacles for the therapeutic agent are viscosity (the anterior portion of vitreous is denser and more viscous) and compositional gradients, which are concerned as the major factors of determining the local differences in concentrations of IVT administered small molecules or vectors.^{38,46,49–51} According to the fundus and confocal images of flat mounts of AAV2-injected eyes in the injection group, which show widespread strong GFP signaling throughout the retina (Figures 3 and 4), the proposed technique allowed the viral vector to traverse the aforementioned barriers. In addition to the uniform distribution of viral vector throughout the retina, the peripapillary injection enabled the viral vector to penetrate deeply to reach the INL, thereby demonstrating enhanced transduction (Figure 5).

Another physical barrier, ILM, that also prevents AAV to reach the retina, was proposed for removal, which may potentially cause retinal damage.^{52–54} Thus, the proposed modulations to circumvent the physical barriers, that is, enzymatic or surgical removal of vitreous and/or ILM,^{19–23} could be considered as two-edged swords, unlike our novel technique using the simple approach with minimal

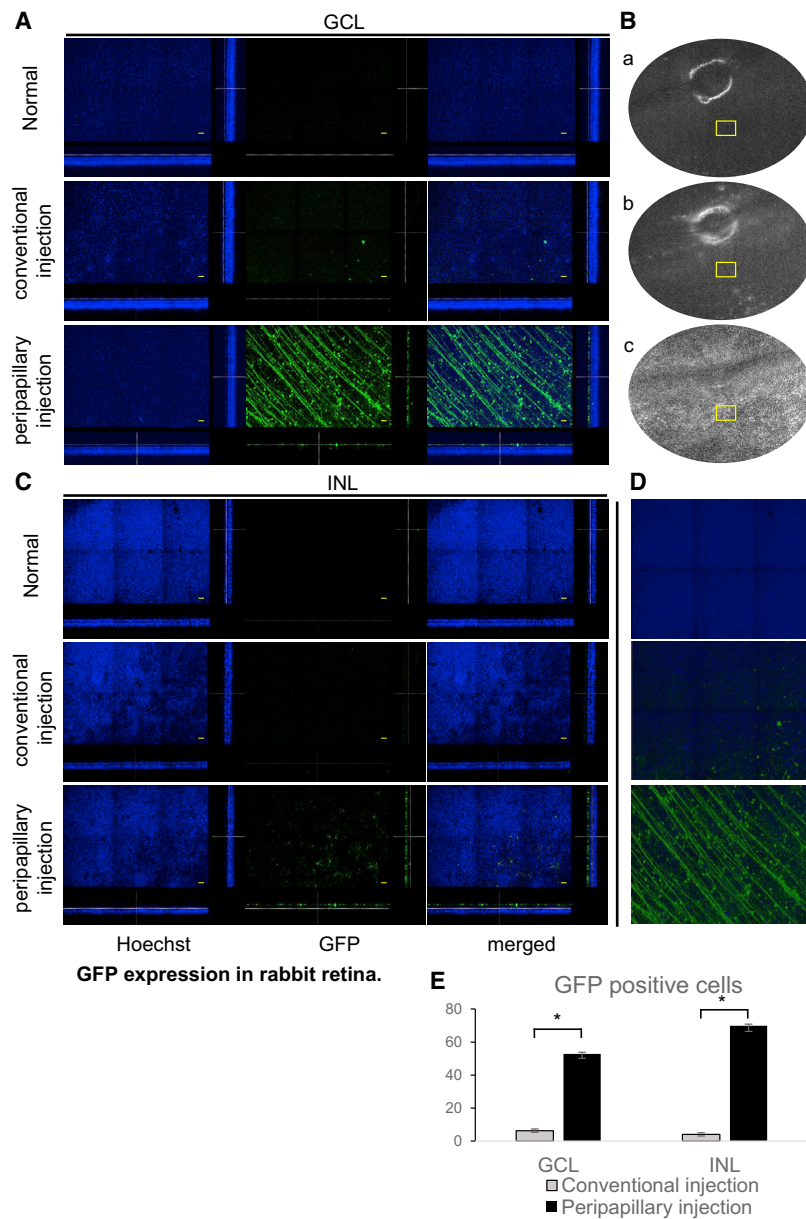


Figure 4. GFP Expression in Rabbit Retina

(A) z stack slides of rabbit retina at the level of ganglion cells. Scale bars, 50 μ m. (B) Representative fundus images of the rabbit retina. (C) z stack slides of rabbit retina at the level of INL. Scale bars, 50 μ m. (D) 3D reconstruction of z stack images of rabbit retina. (E) Quantitative analysis of GFP-expressing cells in GCL and INL of rabbit retina. Bars represent the mean number of GFP-positive cells \pm SEM per field. * $p < 0.01$.

tration in the retina of rabbits in both groups compared with control retinae (Figure 6B). These results indicate that activation of the glia was associated with vector administration, consistent with the results of other studies, which reported temporality of the process without transition to chronic inflammation.^{56–59}

It is generally accepted that intraocular inflammation results in the induction of cytokines in the vitreous cavity along with AH.^{60–62} Therefore, we analyzed AH for the levels of IL-6 and IL-8 (Figure 7). The results of the ELISA assay demonstrated similar levels of cytokines at 4 weeks in both groups of rabbit eyes injected with AAV2 or vehicle. Thus, normal morphology of the retina with trace to mild inflammatory signs of the anterior segment as well as cytokine levels demonstrated that subclinical signs of inflammation might arise after AAV2 administration, and the safety profile of the peripapillary injection technique was found to be the same as for the conventional method.

Taken together, the use of illuminated long-needle attached injection system for IVT administration allows the viral vector to widespread throughout the fundus and penetrate the deeper layers of the retina with dramatically enhanced transduction efficacy than using the conventional method, with a similar safety profile. The novel injection system may serve as an effective tool in experiments with

intervention. Conventional IVT manipulations using an endoilluminator require another additional port; however, our equipment, which uses an illuminated long-needle-attached injection system, allows the surgeon to visualize the fundus and inject the therapeutic agent through the single port, thereby reducing the surgical risk. To assess the safety of the peripapillary injection, we analyzed the tissue for local immune response and AH for cytokine content. Glial cell activation is considered as a local response to any type of neuronal damage.^{9,55} In our study, AAV2 administration in both injection groups resulted in GFAP expression in rabbit retina (Figure 6A), which is normally devoid of GFAP.^{31–33} In addition, Iba1 immunoreactivity was found to be increased upon AAV2 adminis-

large animals and in clinical trials to reach the maximum potential of gene therapy.

MATERIALS AND METHODS

Animal Care

This study was conducted in accordance with the *Guide of the Care and Use of Laboratory Animals* and the Association for Research in Vision and Ophthalmology Statement for the Use of Animals in Ophthalmic and Vision Research, and it was approved by the Institutional Animal Care and Use Committee for Soonchunhyang University Hospital Bucheon. 15 New Zealand White rabbits (male, 2–2.5 kg) were used in this study and housed under standard vivarium

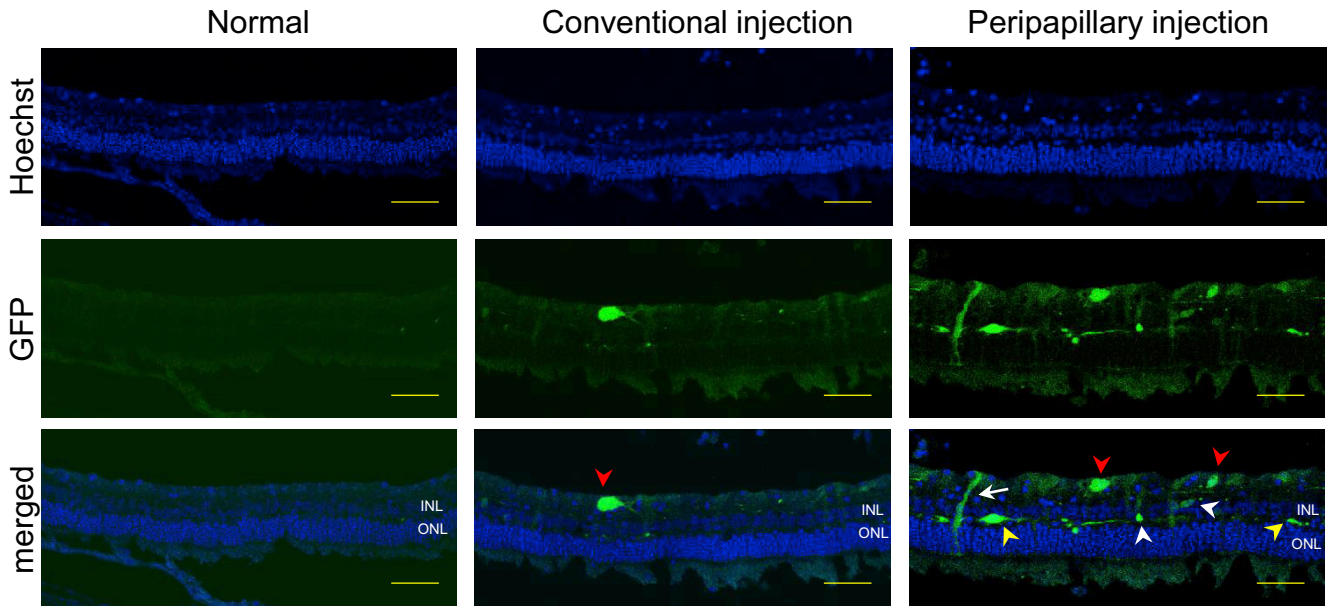


Figure 5. Expression of GFP in Rabbit Retinas at 4 weeks of Injection (Scale Bars, 50 μ m)

conditions (23°C–26°C, 12-h light/12-h dark cycle, food and water provided *ad libitum*). Prior to experimental procedures including ophthalmological examinations, AH collection, and IVT injection, rabbits were anesthetized by subcutaneous injection of a mixture of tiletamine/zolazepam (Zoletil) (3 mg/kg) and xylazine (5 mg/kg).

Grouping and IVT Injection

The animals were randomly grouped into two groups of seven rabbits each. Right eyes of rabbits received 100 μ L (2.11 \times 10¹¹ vector genomes [vg]) of peripapillary IVT injections of recombinant AAV2-CMV-EGFP (Vigene Biosciences, Rockville, MD, USA), and left eyes received 100 μ L of BSS using the same injection method as for right eyes. Seven rabbits (14 eyes) were treated using a novel injection system (Figure 1A). The novel injection system was constructed with optical fiber (OZ Optics, Ottawa, ON, Canada) inside the syringe attached to a 27G needle 25 mm in length. The optical fiber was con-

nected to a 650-nm light source (MBB1F1; Thorlabs, Newton, NJ, USA).

The injection procedure was performed after the induction of general anesthesia, and the eyelids and the conjunctival sac were disinfected by 5% povidone-iodine in BSS. Pupil dilation was achieved with 0.5% tropicamide and 0.5% phenylephrine (Tropherine; Hanmi Pharmaceutical, Seoul, South Korea). Viral vector was injected deep into the vitreous cavity in front of the optic nerve using the novel injection system under a surgical microscope (OPMI Lumera 700; Carl Zeiss, Oberkochen, Germany) (Figure 1B). The conventional method used to treat seven rabbits (14 eyes) was to inject the viral vector or vehicle using a 27G 13-mm needle. One rabbit (both eyes) was treated IVT with 50 μ g of (LPS) and was labeled as the positive controls for AH analysis. The needle was maintained in place for 30 s to allow pressure equilibration.

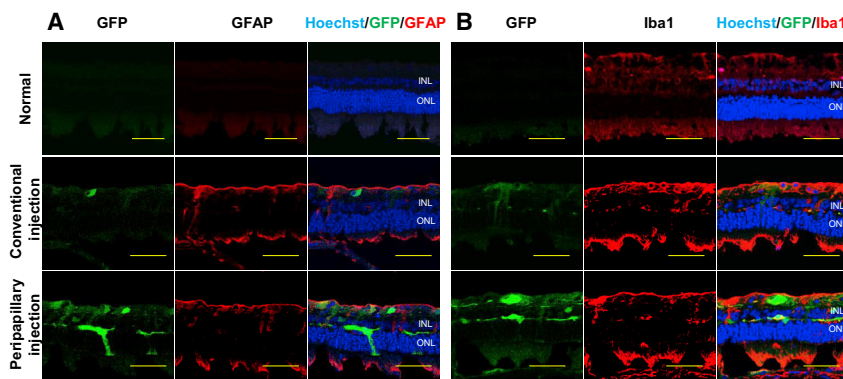


Figure 6. Glial Cell Activation in Transduced Retina

Immunofluorescence staining of rabbit retina for GFAP (A) and Iba1 (B). Scale bars, 50 μ m.

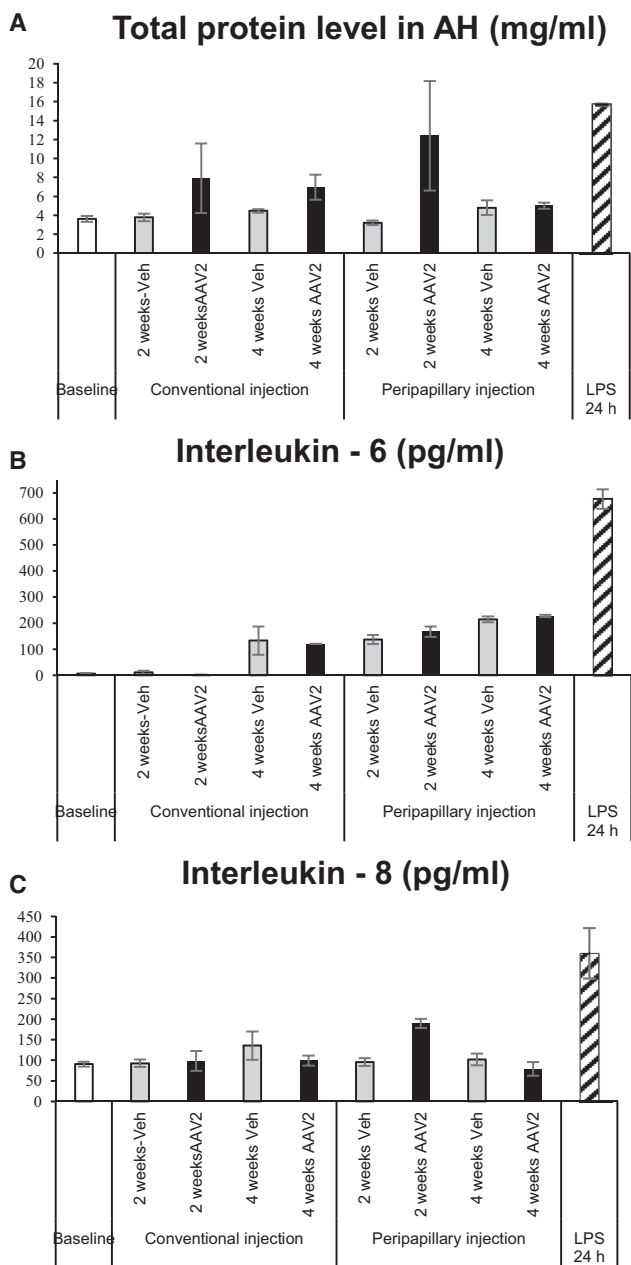


Figure 7. Aqueous Humor Analysis
(A–C) Analyses of total protein level (A), expression of IL-6 (B), and expression of IL-8 (C). Bars represent the mean ± SEM.

Ophthalmological Examinations

All rabbits were examined at baseline and 2 and 4 weeks. Ophthalmological examinations of the rabbit eye included evaluation of conjunctival vessels, vitreous body, and fundus imaging. Conjunctival hyperemia was evaluated by slit-lamp biomicroscopy as described previously with some modifications.⁶³ Briefly, the following scores were used: 0, conjunctiva appeared blanched to reddish pink without perilimbal injection; 1, enlargement of vessels normally visible at the

limbus; 2, branching of vessels at the limbus, new vessels are visible; 3, new vessels visible on bulbar conjunctiva; 4, deep, bright, diffuse redness of conjunctiva. The status of the vitreous was evaluated by slit-lamp biomicroscopy using the grading system as described previously with some modifications.⁶⁴ Briefly, the following scores were used: 0, clearly visible posterior pole; 1, few opacities without obscuration of retinal details; 2, few opacities resulting in slightly blurring of fundus details; 3, significantly blurred retinal details, but distinguishable; 4, fundus details are not visible.

Wide-field fundus images were taken using Optos California (Optos, Dunfermline, Scotland) at baseline and weeks 2 and 4 post-injection. Rabbits were anesthetized followed by dilation of pupils with 0.5% tropicamide and 0.5% phenylephrine. Fundus images were taken in the mode of color and autofluorescence.

Tissue Collection and Preparation

Rabbits were euthanized with CO₂ at 4 weeks of viral vector injection. Enucleated eyes were immersed in 4% paraformaldehyde in PBS for 3 h, followed by removal of the anterior segment of the eye and vitreous body. The eye cup was fixed for an additional 16 h at 4°C. The retina was carefully dissected from the eye cup, mounted on glass slides, and coverslipped. For cryosections, the retina was immersed in 30% sucrose for 24 h for cryoprotection. Furthermore, the eye cup was embedded in OCT compound (Sakura Finetek, Torrance, CA, USA), sectioned at 10 μm, mounted on adhesion microscope slides (HistoBond; Marienfeld-Superior, Lauda-Königshofen, Germany), and stored at -80°C until analysis.

Immunofluorescence Assay

Flat-mount retinas and cryosections were processed for immunofluorescence assay. Flat mounts were rinsed in 0.1% Triton X-100 in PBS and blocked with 5% goat serum in PBS for 2 h. Next, the tissues were exposed to chicken polyclonal GFP antibody (catalog #ab13970, Abcam, Cambridge, UK) in blocking buffer for 48 h at 4°C. After washing with washing buffer, the tissues were incubated in goat anti-chicken IgY H+L (fluorescein isothiocyanate [FITC]; catalog #ab46969, Abcam, Cambridge, UK) for 24 h at room temperature. The nuclear counterstaining was performed with Hoechst 33342 in PBS. The tissues were mounted with fluorescence mounting medium (Dako, Santa Clara, CA, USA). Cryosections of rabbit retina were washed with washing buffer followed by blocking in blocking buffer for 1 h. Furthermore, sections were exposed to primary antibodies (GFP [catalog #ab13970] and Iba1 [catalog #019-19741], Wako, Richmond, VA, USA; GFAP [catalog #12389], Cell Signaling Technology, Danvers, MA, USA) in blocking buffer for 2 h at room temperature. After washing with washing buffer, the tissues were incubated with secondary antibodies (goat anti-chicken IgY H+L [FITC], Abcam, Cambridge, UK and Alexa Fluor 568, Invitrogen, Carlsbad, CA, USA) for 2 h at room temperature. After Hoechst staining and washing, sections were mounted with fluorescence mounting medium. The negative control experiments were carried out in the same manner (Figure S1).

Image Analysis and Cell Counting

Tissue imaging was performed with the use of the Leica SP8 (Leica Microsystems, Wetzlar, Germany) confocal microscope. Six visual fields representing a 1,162.4- μm length and 1,743.6- μm width were randomly sampled from each flat-mounted retina, and serial optical z sectioning was performed. Three-dimensional images were reconstructed using a Leica LAS-X software package. GFP-expressing cells at the level of GCL and INL were manually calculated using ImageJ software (National Institutes of Health, Bethesda, MD, USA).

Aqueous Humor Collection and Analysis

After induction of general anesthesia followed by pre-procedure antisepsis, AH samples were collected with a 30G needle before injection of the viral vector, at weeks 2 and 4 post-injection. The needle was introduced into the anterior chamber through the cornea, and approximately 100 μL of AH was passively extracted. All samples were stored at -80°C until analysis.

Protein concentration was evaluated using a bicinchoninic acid (BCA) kit (Thermo Scientific, Middlesex, MA, USA) according to manufacturers' protocol. The absorbance value at 562 nm was detected using a SpectraMax ABS Plus microplate reader (Molecular Devices, San Jose, CA, USA).

Rabbit AH was assayed for a rabbit IL-6 ELISA kit (MyBioSource, San Diego, CA, USA) with a minimum detection limit of 5 pg/mL and a rabbit IL-8 ELISA kit (Cusabio Technology, Houston, TX, USA) with a minimum detection limit of 23.5 pg/mL according to the manufacturer's protocol. The absorbance value at 450 nm was detected using a SpectraMax ABS Plus microplate reader (Molecular Devices, San Jose, CA, USA).

Statistical Analysis

The repeated-measures ANOVA was used to compare the differences in clinical signs of inflammation. An independent sample t test was used to evaluate the differences in GFP-expressing cell numbers between groups. The Kruskal-Wallis test with *post hoc* analysis was used to calculate the statistical significance of differences among groups in aqueous humor analysis. Statistical analysis was performed with the IBM SPSS Statistics software (version 22, IBM, Armonk, NY, USA). Differences were considered statistically significant when $p \leq 0.05$.

SUPPLEMENTAL INFORMATION

Supplemental Information can be found online at <https://doi.org/10.1016/j.omtm.2020.03.018>.

AUTHOR CONTRIBUTIONS

Conceptualization, T.K.P.; Methodology, T.K.P. and S.B.M.; Validation, T.K.P. and S.B.M.; Formal analysis, S.B.M. and J.Y.Y.; Investigation, S.B.M. and J.Y.Y.; Resources, T.K.P.; Writing – Original Draft, S.B.M.; Writing – Review & Editing, T.K.P., S.B.M., D.H.A., and J.W.H.; Visualization, S.B.M., J.Y.Y., and T.H.H.; Supervision,

T.K.P.; Project Administration, T.K.P.; Funding Acquisition, T.K.P. All authors read and approved the final manuscript.

COMPETING INTERESTS

The authors declare no competing interests.

ACKNOWLEDGMENTS

This research was supported by a grant of the Korea Health Technology R&D Project through the Korea Health Industry Development Institute (KHIDI), funded by the Ministry of Health and Welfare, Republic of Korea (grant no. HI17C0966), and by Basic Science Research Program through the National Research Foundation of Korea (NRF) funded by the Ministry of Science and ICT (grant no. 2019R1A2C1005055).

REFERENCES

- Bainbridge, J.W.B., Mehat, M.S., Sundaram, V., Robbie, S.J., Barker, S.E., Ripamonti, C., Georgiadis, A., Mowat, F.M., Beattie, S.G., Gardner, P.J., et al. (2015). Long-term effect of gene therapy on Leber's congenital amaurosis. *N. Engl. J. Med.* *372*, 1887–1897.
- Cideciyan, A.V., Aleman, T.S., Boye, S.L., Schwartz, S.B., Kaushal, S., Roman, A.J., Pang, J.J., Sumaroka, A., Windsor, E.A., Wilson, J.M., et al. (2008). Human gene therapy for RPE65 isomerase deficiency activates the retinoid cycle of vision but with slow rod kinetics. *Proc. Natl. Acad. Sci. USA* *105*, 15112–15117.
- Ghazi, N.G., Abboud, E.B., Nowilaty, S.R., Alkuraya, H., Alhommadi, A., Cai, H., Hou, R., Deng, W.T., Boye, S.L., Almaghamsi, A., et al. (2016). Treatment of retinitis pigmentosa due to *MERTK* mutations by ocular subretinal injection of adeno-associated virus gene vector: results of a phase I trial. *Hum. Genet.* *135*, 327–343.
- MacLaren, R.E., Groppe, M., Barnard, A.R., Cottrill, C.L., Tolmachova, T., Seymour, L., Clark, K.R., Doring, M.J., Cremers, F.P., Black, G.C., et al. (2014). Retinal gene therapy in patients with choroideremia: initial findings from a phase 1/2 clinical trial. *Lancet* *383*, 1129–1137.
- Lam, B.L., Davis, J.L., Gregori, N.Z., MacLaren, R.E., Girach, A., Verriotto, J.D., Rodriguez, B., Rosa, P.R., Zhang, X., and Feuer, W.J. (2019). Choroideremia gene therapy phase 2 clinical trial: 24-month results. *Am. J. Ophthalmol.* *197*, 65–73.
- Dimopoulos, I.S., Hoang, S.C., Radziwon, A., Binczyk, N.M., Seabra, M.C., MacLaren, R.E., Somani, R., Tennant, M.T.S., and MacDonald, I.M. (2018). Two-year results after AAV2-mediated gene therapy for choroideremia: the Alberta experience. *Am. J. Ophthalmol.* *193*, 130–142.
- Rakoczy, E.P., Lai, C.M., Magno, A.L., Wikstrom, M.E., French, M.A., Pierce, C.M., Schwartz, S.D., Blumenkranz, M.S., Chalberg, T.W., Degli-Esposti, M.A., and Constable, I.J. (2015). Gene therapy with recombinant adeno-associated vectors for neovascular age-related macular degeneration: 1 year follow-up of a phase 1 randomized clinical trial. *Lancet* *386*, 2395–2403.
- Ginn, S.L., Amaya, A.K., Alexander, I.E., Edelstein, M., and Abedi, M.R. (2018). Gene therapy clinical trials worldwide to 2017: an update. *J. Gene Med.* *20*, e3015.
- Willett, K., and Bennett, J. (2013). Immunology of AAV-mediated gene transfer in the eye. *Front. Immunol.* *4*, 261.
- Anand, V., Duffy, B., Yang, Z., Dejneka, N.S., Maguire, A.M., and Bennett, J. (2002). A deviant immune response to viral proteins and transgene product is generated on subretinal administration of adenovirus and adeno-associated virus. *Mol. Ther.* *5*, 125–132.
- Jacobson, S.G., Cideciyan, A.V., Ratnakaram, R., Heon, E., Schwartz, S.B., Roman, A.J., Peden, M.C., Aleman, T.S., Boye, S.L., Sumaroka, A., et al. (2012). Gene therapy for Leber congenital amaurosis caused by *RPE65* mutations: safety and efficacy in 15 children and adults followed up to 3 years. *Arch. Ophthalmol.* *130*, 9–24.
- Grzybowski, A., Told, R., Sacu, S., Bandello, F., Moisseiev, E., Loewenstein, A., and Schmidt-Erfurth, U.; Euretina Board (2018). 2018 update on intravitreal injections: Euretina expert consensus recommendations. *Ophthalmologica* *239*, 181–193.

13. Ochakovski, G.A., Bartz-Schmidt, K.U., and Fischer, M.D. (2017). Retinal gene therapy: surgical vector delivery in the translation to clinical trials. *Front. Neurosci.* *11*, 174.
14. Marangoni, D., Wu, Z., Wiley, H.E., Zeiss, C.J., Vijayasathay, C., Zeng, Y., Hiriyanna, S., Bush, R.A., Wei, L.L., Colosi, P., and Sieving, P.A. (2014). Preclinical safety evaluation of a recombinant AAV8 vector for X-linked retinoschisis after intravitreal administration in rabbits. *Hum. Gene Ther. Clin. Dev.* *25*, 202–211.
15. MacLachlan, T.K., Lukason, M., Collins, M., Munger, R., Isenberger, E., Rogers, C., Malatos, S., Dufresne, E., Morris, J., Calcedo, R., et al. (2011). Preclinical safety evaluation of AAV2-sFLT01—a gene therapy for age-related macular degeneration. *Mol. Ther.* *19*, 326–334.
16. Guy, J., Qi, X., Koilkonda, R.D., Arguello, T., Chou, T.H., Ruggeri, M., Porciatti, V., Lewin, A.S., and Hauswirth, W.W. (2009). Efficiency and safety of AAV-mediated gene delivery of the human ND4 complex I subunit in the mouse visual system. *Invest. Ophthalmol. Vis. Sci.* *50*, 4205–4214.
17. Chatziralli, I., Nicholson, L., Sivaprasad, S., and Hykin, P. (2015). Intravitreal steroid and anti-vascular endothelial growth agents for the management of retinal vein occlusion: evidence from randomized trials. *Expert Opin. Biol. Ther.* *15*, 1685–1697.
18. Logan, S.A., Weng, C.Y., and Carvounis, P.E. (2016). Intravitreal steroid implants in the management of retinal disease and uveitis. *Int. Ophthalmol. Clin.* *56*, 127–149.
19. Dalkara, D., Kolstad, K.D., Caporale, N., Visel, M., Klimczak, R.R., Schaffer, D.V., and Flannery, J.G. (2009). Inner limiting membrane barriers to AAV-mediated retinal transduction from the vitreous. *Mol. Ther.* *17*, 2096–2102.
20. Cehajic-Kapetanovic, J., Le Goff, M.M., Allen, A., Lucas, R.J., and Bishop, P.N. (2011). Glycosidic enzymes enhance retinal transduction following intravitreal delivery of AAV2. *Mol. Vis.* *17*, 1771–1783.
21. Takahashi, K., Igarashi, T., Miyake, K., Kobayashi, M., Yaguchi, C., Iijima, O., Yamazaki, Y., Kataaki, Y., Miyake, N., Kameya, S., et al. (2017). Improved intravitreal AAV-mediated inner retinal gene transduction after surgical internal limiting membrane peeling in cynomolgus monkeys. *Mol. Ther.* *25*, 296–302.
22. Cehajic-Kapetanovic, J., Milosavljevic, N., Bedford, R.A., Lucas, R.J., and Bishop, P.N. (2017). Efficacy and safety of glycosidic enzymes for improved gene delivery to the retina following intravitreal injection in mice. *Mol. Ther. Methods Clin. Dev.* *9*, 192–202.
23. Tshilenge, K.-T., Ameline, B., Weber, M., Mendes-Madeira, A., Nedellec, S., Biget, M., Provost, N., Libeau, L., Blouin, V., Deschamps, J.Y., et al. (2016). Vitrectomy before intravitreal injection of AAV2/2 vector promotes efficient transduction of retinal ganglion cells in dogs and nonhuman primates. *Hum. Gene Ther. Methods* *27*, 122–134.
24. Baldo, B.A. (2015). Enzymes approved for human therapy: indications, mechanisms and adverse effects. *BioDrugs* *29*, 31–55.
25. Fahim, A.T., Khan, N.W., and Johnson, M.W. (2014). Acute panretinal structural and functional abnormalities after intravitreal ocriplasmin injection. *JAMA Ophthalmol.* *132*, 484–486.
26. Lee, S.H., Colosi, P., Lee, H., Ohn, Y.H., Kim, S.W., Kwak, H.W., and Park, T.K. (2014). Laser photocoagulation enhances adeno-associated viral vector transduction of mouse retina. *Hum. Gene Ther. Methods* *25*, 83–91.
27. Hubschman, J.P., Coffee, R.E., Bourges, J.L., Yu, F., and Schwartz, S.D. (2010). Experimental model of intravitreal injection techniques. *Retina* *30*, 167–173.
28. Rodrigues, E.B., Grumann, A., Jr., Penha, F.M., Shiroma, H., Rossi, E., Meyer, C.H., Stefano, V., Maia, M., Magalhaes, O., Jr., and Farah, M.E. (2011). Effect of needle type and injection technique on pain level and vitreal reflux in intravitreal injection. *J. Ocul. Pharmacol. Ther.* *27*, 197–203.
29. De Stefano, V.S., Abechain, J.J., de Almeida, L.F., Verginassi, D.M., Rodrigues, E.B., Freymuller, E., Maia, M., Magalhaes, O., Nguyen, Q.D., and Farah, M.E. (2011). Experimental investigation of needles, syringes and techniques for intravitreal injections. *Clin. Exp. Ophthalmol.* *39*, 236–242.
30. Haas, P., Falkner-Radler, C., Wimpissinger, B., Malina, M., and Binder, S. (2016). Needle size in intravitreal injections—pain evaluation of a randomized clinical trial. *Acta Ophthalmol.* *94*, 198–202.
31. Schnitzer, J. (1985). Distribution and immunoreactivity of glia in the retina of the rabbit. *J. Comp. Neurol.* *240*, 128–142.
32. Francke, M., Faude, F., Pannicke, T., Bringmann, A., Eckstein, P., Reichelt, W., Wiedemann, P., and Reichenbach, A. (2001). Electrophysiology of rabbit Müller (glial) cells in experimental retinal detachment and PVR. *Invest. Ophthalmol. Vis. Sci.* *42*, 1072–1079.
33. Yoshida, A., Ishiguro, S., and Tamai, M. (1993). Expression of glial fibrillary acidic protein in rabbit Müller cells after lensectomy-vitrectomy. *Invest. Ophthalmol. Vis. Sci.* *34*, 3154–3160.
34. Shi, H., Gao, J., Pei, H., Liu, R., Hu, W.K., Wan, X., Li, T., and Li, B. (2012). Adeno-associated virus-mediated gene delivery of the human ND4 complex I subunit in rabbit eyes. *Clin. Exp. Ophthalmol.* *40*, 888–894.
35. Doi, K., Kong, J., Hargitai, J., Goff, S.P., and Gouras, P. (2004). Transient immunosuppression stops rejection of virus-transduced enhanced green fluorescent protein in rabbit retina. *J. Virol.* *78*, 11327–11333.
36. Igarashi, T., Miyake, K., Asakawa, N., Miyake, N., Shimada, T., and Takahashi, H. (2013). Direct comparison of administration routes for AAV8-mediated ocular gene therapy. *Curr. Eye Res.* *38*, 569–577.
37. Li, Q., Miller, R., Han, P.-Y., Pang, J., Dinculescu, A., Chiodo, V., and Hauswirth, W.W. (2008). Intraocular route of AAV2 vector administration defines humoral immune response and therapeutic potential. *Mol. Vis.* *14*, 1760–1769.
38. Liang, F.-Q., Aleman, T.S., Dejneka, N.S., Dudas, L., Fisher, K.J., Maguire, A.M., Jacobson, S.G., and Bennett, J. (2001). Long-term protection of retinal structure but not function using RAAV.CNTF in animal models of retinitis pigmentosa. *Mol. Ther.* *4*, 461–472.
39. Auricchio, A., Kobinger, G., Anand, V., Hildinger, M., O'Connor, E., Maguire, A.M., Wilson, J.M., and Bennett, J. (2001). Exchange of surface proteins impacts on viral vector cellular specificity and transduction characteristics: the retina as a model. *Hum. Mol. Genet.* *10*, 3075–3081.
40. Hellström, M., Ruitenberg, M.J., Pollett, M.A., Ehlert, E.M., Twisk, J., Verhaagen, J., and Harvey, A.R. (2009). Cellular tropism and transduction properties of seven adeno-associated viral vector serotypes in adult retina after intravitreal injection. *Gene Ther.* *16*, 521–532.
41. Büning, H., Huber, A., Zhang, L., Meumann, N., and Hacker, U. (2015). Engineering the AAV capsid to optimize vector-host-interactions. *Curr. Opin. Pharmacol.* *24*, 94–104.
42. Sullivan, J.A., Stanek, L.M., Lukason, M.J., Bu, J., Osmond, S.R., Barry, E.A., O'Riordan, C.R., Shihabuddin, L.S., Cheng, S.H., and Scaria, A. (2018). Rationally designed AAV2 and AAVrh8R capsids provide improved transduction in the retina and brain. *Gene Ther.* *25*, 205–219.
43. Klimczak, R.R., Koerber, J.T., Dalkara, D., Flannery, J.G., and Schaffer, D.V. (2009). A novel adeno-associated viral variant for efficient and selective intravitreal transduction of Rat Müller cells. *PLoS ONE* *4*, e7467.
44. Peeters, L., Sanders, N.N., Braeckmans, K., Boussey, K., Van de Voorde, J., De Smedt, S.C., and Demeester, J. (2005). Vitreous: a barrier to nonviral ocular gene therapy. *Invest. Ophthalmol. Vis. Sci.* *46*, 3553–3561.
45. Pitkänen, L., Rupunen, M., Nieminen, J., and Urtti, A. (2003). Vitreous is a barrier in nonviral gene transfer by cationic lipids and polymers. *Pharm. Res.* *20*, 576–583.
46. Kleinberg, T.T., Tzekov, R.T., Stein, L., Ravi, N., and Kaushal, S. (2011). Vitreous substitutes: a comprehensive review. *Surv. Ophthalmol.* *56*, 300–323.
47. Dudas, L., Anand, V., Acland, G.M., Chen, S.J., Wilson, J.M., Fisher, K.J., Maguire, A.M., and Bennett, J. (1999). Persistent transgene product in retina, optic nerve and brain after intraocular injection of rAAV. *Vision Res.* *39*, 2545–2553.
48. Mowat, F.M., Gornik, K.R., Dinculescu, A., Boye, S.L., Hauswirth, W.W., Petersen-Jones, S.M., and Bartoe, J.T. (2014). Tyrosine capsid-mutant AAV vectors for gene delivery to the canine retina from a subretinal or intravitreal approach. *Gene Ther.* *21*, 96–105.
49. Friedrich, S., Cheng, Y.L., and Saville, B. (1997). Finite element modeling of drug distribution in the vitreous humor of the rabbit eye. *Ann. Biomed. Eng.* *25*, 303–314.
50. Stay, M.S., Xu, J., Randolph, T.W., and Barocas, V.H. (2003). Computer simulation of convective and diffusive transport of controlled-release drugs in the vitreous humor. *Pharm. Res.* *20*, 96–102.
51. Maurice, D. (2001). Review: practical issues in intravitreal drug delivery. *J. Ocul. Pharmacol. Ther.* *17*, 393–401.

52. Haritoglou, C., Gandorfer, A., and Kampik, A. (2004). Internal limiting membrane peeling. *Ophthalmology* *111*, 1791–1792.
53. Steven, P., Laqua, H., Wong, D., and Hoerauf, H. (2006). Secondary paracentral retinal holes following internal limiting membrane removal. *Br. J. Ophthalmol.* *90*, 293–295.
54. Hisatomi, T., Notomi, S., Tachibana, T., Sassa, Y., Ikeda, Y., Nakamura, T., Ueno, A., Enaida, H., Murata, T., Sakamoto, T., and Ishibashi, T. (2014). Ultrastructural changes of the vitreoretinal interface during long-term follow-up after removal of the internal limiting membrane. *Am. J. Ophthalmol.* *158*, 550–556.e1.
55. de Hoz, R., Rojas, B., Ramírez, A.I., Salazar, J.J., Gallego, B.I., Triviño, A., and Ramírez, J.M. (2016). Retinal macroglial responses in health and disease. *BioMed Res. Int.* *2016*, 2954721.
56. Ramachandran, P.S., Lee, V., Wei, Z., Song, J.Y., Casal, G., Cronin, T., Willett, K., Huckfeldt, R., Morgan, J.I., Aleman, T.S., et al. (2017). Evaluation of dose and safety of AAV7m8 and AAV8BP2 in the non-human primate retina. *Hum. Gene Ther.* *28*, 154–167.
57. Giove, T.J., Sena-Esteves, M., and Eldred, W.D. (2010). Transduction of the inner mouse retina using AAVrh8 and AAVrh10 via intravitreal injection. *Exp. Eye Res.* *91*, 652–659.
58. Reimsnider, S., Manfredsson, F.P., Muzyczka, N., and Mandel, R.J. (2007). Time course of transgene expression after intrastriatal pseudotyped rAAV2/1, rAAV2/2, rAAV2/5, and rAAV2/8 transduction in the rat. *Mol. Ther.* *15*, 1504–1511.
59. Lowenstein, P.R., Mandel, R.J., Xiong, W.D., Kroeger, K., and Castro, M.G. (2007). Immune responses to adenovirus and adeno-associated vectors used for gene therapy of brain diseases: the role of immunological synapses in understanding the cell biology of neuroimmune interactions. *Curr. Gene Ther.* *7*, 347–360.
60. Wakefield, D., and Lloyd, A. (1992). The role of cytokines in the pathogenesis of inflammatory eye disease. *Cytokine* *4*, 1–5.
61. Murray, P.I., Hoekzema, R., van Haren, M.A., de Hon, F.D., and Kijlstra, A. (1990). Aqueous humor interleukin-6 levels in uveitis. *Invest. Ophthalmol. Vis. Sci.* *31*, 917–920.
62. Perez, V.L., Papaliodis, G.N., Chu, D., Anzaar, F., Christen, W., and Foster, C.S. (2004). Elevated levels of interleukin 6 in the vitreous fluid of patients with pars planitis and posterior uveitis: the Massachusetts eye & ear experience and review of previous studies. *Ocul. Immunol. Inflamm.* *12*, 193–201.
63. Van de Velde, S., Van Bergen, T., Sijnave, D., Hollanders, K., Castermans, K., Defert, O., Leysen, D., Vandewalle, E., Moons, L., and Stalmans, I. (2014). AMA0076, a novel, locally acting Rho kinase inhibitor, potently lowers intraocular pressure in New Zealand white rabbits with minimal hyperemia. *Invest. Ophthalmol. Vis. Sci.* *55*, 1006–1016.
64. Nussenblatt, R.B., Palestine, A.G., Chan, C.-C., and Roberge, F. (1985). Standardization of vitreal inflammatory activity in intermediate and posterior uveitis. *Ophthalmology* *92*, 467–471.